Structural Engineering and Mechanics, *Vol. 74, No. 1 (2020) 55-67*
DOI: https://doi.org/10.12989/sem.2020.74.1.055

Extreme value modeling of structural load effects with non-identical distribution using clustering

Junyong Zhou[1a], Xin Ruan[2b], Xuefei Shi[*2] and Chudong Pan[1c]

[1]*School of Civil Engineering, Guangzhou University, 230 West Waihuan Road, Guangzhou, Guangdong 510006, China.*
[2]*Department of Bridge Engineering, Tongji University, 1239 Siping Road, Shanghai 200092, China*

(Received March 11, 2019, Revised October 19, 2019, Accepted November 12, 2019)

Abstract. The common practice to predict the characteristic structural load effects (LEs) in long reference periods is to employ the extreme value theory (EVT) for building limit distributions. However, most applications ignore that LEs are driven by multiple loading events and thus do not have the identical distribution, a prerequisite for EVT. In this study, we propose the composite extreme value modeling approach using clustering to (a) cluster initial blended samples into finite identical distributed subsamples using the finite mixture model, expectation-maximization algorithm, and the Akaike information criterion; (b) combine limit distributions of subsamples into a composite prediction equation using the generalized Pareto distribution based on a joint threshold. The proposed approach was validated both through numerical examples with known solutions and engineering applications of bridge traffic LEs on a long-span bridge. The results indicate that a joint threshold largely benefits the composite extreme value modeling, many appropriate tail approaching models can be used, and the equation form is simply the sum of the weighted models. In numerical examples, the proposed approach using clustering generated accurate extrema prediction of any reference period compared with the known solutions, whereas the common practice of employing EVT without clustering on the mixture data showed large deviations. Real-world bridge traffic LEs are driven by multi-events and present multipeak distributions, and the proposed approach is more capable of capturing the tendency of tailed LEs than the conventional approach. The proposed approach is expected to have wide applications to general problems such as samples that are driven by multiple events and that do not have the identical distribution.

Keywords: structural load effect; extreme value modeling; clustering; non-identical distribution; peaks over threshold; generalized Pareto distribution

1. Introduction

Variable actions such as traffic, wind, and temperature have a significant effect on structures. Because of the adverse environmental impacts and aging structures, the precise estimation of load effect (LE) under variable actions over the lifetime of a structure is particularly important and can contribute to the optimal resource allocation of maintenance and management for infrastructures (Frangopol and Liu 2007, Au-Yong *et al*. 2017, Zhou *et al*. 2019). To ensure safety in the design or assessment of structures, the specified reference period for variable action is generally very long. For example, the return periods for traffic load on bridges in the Chinese design code (MCT 2015) and the Eurocode 1 (EC1 2003) are 1950 years and 1000 years, respectively. However, knowledge of the effect of variable actions on structures is limited because they are highly random and measurements are generally short-dated. The common practice is to infer the characteristic value of long return periods based on available measurements or simulations, which is the scope of extreme value statistics (Gumbel 2012).

1.1 Classical extreme value theory

The classical extreme value theory (EVT) aims to build statistical models to identify the limit distribution for the maximum and minimum values based on the underlying data. In EVT, two classes of extreme value distributions are used to find an accurate limit. The first class is known as the generalized extreme value (GEV) distribution based on block maxima (BM) or minima (Gumbel 2012), and the second is the generalized Pareto distribution (GPD) based on peaks over thresholds (POT) (Davison and Smith 1990). These two theories are widely used in the research of lifetime structural LEs under the loading of traffic, wind, temperature, or wave (Zhou *et al*. 2018b, Ye *et al*. 2017, Easterling *et al*. 2000, Jeong *et al*. 2016, Xia and Ni 2016). Moreover, it was reported that the POT theory took more information on local extrema from limited underlying data and shown more accurate estimates than the BM theory in some engineering fields (Rivas *et al*. 2008, Madsen *et al*. 1997). In this paper, we choose the POT theory based extrapolation method for further study.

With a sequence of independent and identically distributed observations X_i (i=1,2,…,m), Davison and Smith

*Corresponding author, Professor
E-mail: zhoujunyong_fly@163.com
[a] Ph.D.
E-mail: jyzhou@gzhu.edu.cn
[b] Professor
E-mail: ruanxin@tongji.edu.cn
[c] Ph.D.
E-mail: panchudong@gzhu.edu.cn

http://www.techno-press.com/journals/sem&subpage=7
ISSN: 1225-4568 (Print), 1598-6217 (Online)

(1990) showed that the excess y=X-u over a certain high threshold u can be approximated by GPD

$$\begin{aligned} F_u(y) &= \Pr(X \le y+u | X > u) = \frac{F(y+u)-F(u)}{1-F(u)} \\ &= G(x;\xi,u,\sigma) = 1-\left[1+\xi\left(\frac{x-u}{\sigma}\right)\right]^{-1/\xi}. \end{aligned} \quad (1)$$

where F(.) is the probability distribution function of these observations; F_u(.) is the probability distribution function of these excesses; ξ, u, σ are the shape, location, and scale parameters of the GPD, respectively. The GPD is defined on the optimal threshold u. The shape parameter ξ shows the tail behavior of the GPD and keeps stable when the threshold changes. The scale parameter σ is closely related to the choice of threshold such that $\sigma'=\sigma+\xi(u'-u)$, where u' and σ' are the new threshold and the scale parameter, respectively.

A critical prerequisite for the application of EVT is that the underlying data for BM or the exceedance data for POT should follow the identical independent distribution (iid). However, real-world structural LEs do not necessarily follow this hypothesis, and this fact is ignored in most studies, which may lead to significant overestimation or underestimation of lifetime LEs. In practice, structural LEs subjected to a certain variable action (such as traffic) are multimodally distributed driven by multiple loading events. Some loading events have a large probability of occurrence but generate low LEs, while some events produce large LEs but their probabilities of occurrence are relatively low, such as bridge traffic loading effects induced by free flow and congested flow (Caprani 2012, Ruan *et al.* 2017a). Furthermore, several parallel loading events may jointly produce adverse LEs, such as structural wind loading effects induced by thunderstorms and hurricanes (Gomes and Vickery 1978, Zhang et al. 2018). Over the structure's lifetime, these loading events may concurrently contribute to the prediction of extreme LEs. Therefore, the real-world LEs are the combination of the results of many loading events and do not have identical distributions.

1.2 Composite extreme extrapolation approach

On non-identical samples based extreme extrapolation, Gomes and Vickery (1978) reported that extreme wind speed can be generated by several wind climates such as extensive pressure system storms, thunderstorms, and hurricanes. Each wind climate represents a certain mechanism, and the samples are assumed to follow the iid distribution, and therefore are modeled using the classical EVT. However, mixed samples from more than one mechanism are not identically distributed; thus, a method of "composite extreme wind speed diagram," which yields more accurate probability estimates than the traditional Gumbel (GEV type I) extrapolation, has been proposed. The Gomes and Vickery approach has been widely applied in wind engineering (Zhang *et al*. 2018, Cook 2004). For an analogous problem of extreme traffic loading effect on short- to medium-span bridges, Caprani *et al.* (2008) divided the traffic loading events that govern extreme LEs into several mechanisms, i.e., the number of trucks involved, and used the composite distribution statistics method to predict the characteristic values over the lifetime of a bridge. The work were motivated by the Gomes and Vickery approach, where the composite modeling function is derived theoretically based on GEV fitting on each mechanism-governed subsample using BM. Zhou *et al.* (2016) studied the same problem as Caprani *et al.* (2008) did but used the mixture peaks-over-threshold approach to predict the characteristic values. The outline of the mixture peaks-over-threshold approach (or composite distribution statistics method) is given as follows.: (1) identify and classify the bridge traffic LEs by known event types, i.e., the number of trucks involved; (2) pick the featured LEs of each event type using the POT (or BM) method; (3) construct the limit distribution of GPD (or GEV) for featured LEs of each event type; (4) combine these GPD (or GEV) distributions of event types to obtain the composite method of prediction. The composite extreme extrapolation using the BM or the POT theory follows the same concepts, and this study focuses on the POT theory.

On mixture observations from K mechanisms, single-mechanism-governed subsamples are assumed to be described by an identical distribution, and their POT can be approximated by a GPD based on the classical EVT. Zhou *et al.* (2016) assumed that the survivor function, i.e., the probability of the underlying data larger than a certain value (over threshold), x, for these mixed observations, could be formulated with composite GPD.

$$\begin{aligned} P(X>x) &= \sum_{k=1}^{K} w_k\left[1-F_k(x)\right] \\ &= \sum_{k=1}^{K} w_k\left[1-F_k(u_k)\right]\left[1-G_k(x;\xi_k,u_k,\sigma_k)\right]. \end{aligned} \quad (2)$$

where F_k(.) is the probability distribution function of the kth-mechanism-governed subsamples; G_k(.) is the corresponding GPD distribution for F_k(.); ξ_k, u_k, σ_k are the shape, location, and scale parameters of G_k(.), respectively.

The studies reviewed in this section (Gomes and Vickery 1978, Zhang *et al*. 2018, Cook 2004, Caprani *et al.* 2008, Zhou *et al.* 2016) are built on two prerequisites: (1) the mechanisms governing the extreme values are assumed to be identifiable; (2) observations in the same mechanisms are assumed to follow an identical distribution. These two conditions are acceptable for the problems investigated in those studies and therefore the LEs can be easily separated. However, in most real-world problems, the governed mechanisms of extreme values are generally unknown or numerous, and the underlying data are blended. For example, critical traffic loading events for long-span bridges are many, including free flow with high traffic volumes or high truck proportions and congested flow of various forms, and thus difficult to differentiate. However, the structural LEs in an assumed mechanism do not strictly follow an identical distribution. For instance, bridge LEs from the single-truck loading event are assumed to follow iid in current studies (Caprani *et al*. 2008, Zhou *et al*. 2016). However, it was reported that truck had many types and the bridge LEs under a single truck but of different truck types were multimodally distributed (Zhou *et al.* 2018b, Tabsh and Mitchell 2016, Ruan *et al*. 2017b).

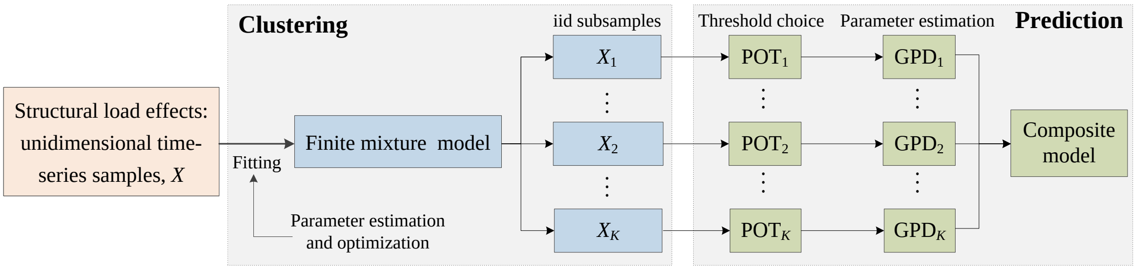

Fig. 1. Framework of the proposed approach

1.3 Contribution

This study proposes a framework for extreme value modeling of non-identical samples using clustering. The framework employs the POT theory to address the extrapolation problem of multi-event-driven structural LEs that are generated by unknown or numerous mechanisms and that do not accord with the iid assumption. Using clustering, initial blended non-identical samples are automatically categorized into several identical subsamples without assuming that the governing mechanisms are identifiable. Therefore, the approach is general and simple for use.

The framework contains two parts: (1) cluster the initial blended samples into several iid subsamples based on the finite mixture model, expectation-maximization (EM) algorithm, and Akaike information criterion (AIC); (2) build the limit distribution of GPD based on the POT of each iid subsample, and combine these GPD models into a composite prediction equation. This framework was developed based on the work of Caprani *et al*. (2008) and Zhou *et al*. (2016). However, it further showed that a joint threshold largely benefits and simplifies the prediction equation. Numerical examples with known solutions are conducted to verify the framework of the composite extreme value modeling using clustering. Finally, the engineering application of the proposed approach is demonstrated on structural LEs of traffic loading on a long-span bridge. The distribution functions of realistic engineering problems are unknown, and thus the theoretical solution for prediction is undefined. The proposed approach is more accurate to capture the tail tendency of real-world data than the conventional direct application of EVT without clustering. Furthermore, the choice of the type of the finite mixture model for clustering is discussed.

2. Approach

2.1 Framework

LE is the structural response (such as displacement, internal force, or stress) in a continuous period of time under loading. Structural LEs in a specific direction can be regarded as unidimensional time-series samples. On given structural LEs that are not identically distributed, the framework of the approach is shown in Fig. 1. The approach first clusters the initial samples into finite subsamples that accord with the iid assumption, where the finite mixture model is used to fit and separate the subsamples. The traditional POT-based GPD approach is employed to build the limit distribution for each iid subsample, and these limit distributions are then combined to form the composite prediction equation.

2.2 Clustering non-identical samples

To categorize the initial samples into finite identical distributed subsamples, the finite mixture model is used as the target multimodal distribution. Then, the EM algorithm is employed to estimate the parameters in the finite mixture model. Finally, AIC is applied to determine the optimal number of model components used for clustering.

2.2.1 Finite mixture model

The initial unidimensional time-series samples, X, can be described by a finite mixture model

$$f\left(x \mid \vec{\theta}\right)=\sum_{k=1}^{K} w_k \cdot f_k\left(x \mid \vec{\theta}_k\right). \tag{3}$$

where K represents the number of models used; $\overrightarrow{\theta_k}$ is the parameter of the kth model component; $f(.)$ is the probability density function of X; w_k and $f_k(x|\overrightarrow{\theta_k})$ are the weight coefficient and the probability density function of the kth model component, respectively. These weight coefficients obey the constraint of $\sum_{k=1}^{K} w_k = 1$.

In this manner, these variables can be clustered into finite sets of iid subsamples as $X_k(k=1,2,\ldots,K)$, where the density function of X_k is $f_k(x|\overrightarrow{\theta_k})$. In mixture modeling, the same or different types of models can be used. The Gaussian mixture model can well describe most engineering situations (McLachlan and Peel 2004), and the Gumbel distribution can well describe the tail tendency of many structural LEs (Gomes and Vickery 1978). Therefore, the Gaussian mixture model and the Gumbel mixture model, shown in Eqs. (4) and (5), respectively, are compared to investigate the sensitivity of the type of the finite mixture model selected.

$$f\left(x \mid \vec{\theta}\right)=\sum_{k=1}^{K} w_k \cdot \frac{1}{\sqrt{2\pi\Sigma_k}} \exp\left[-\frac{\left(x-\mu_k\right)^2}{2\Sigma_k}\right]. \tag{4}$$

$$f\left(x \mid \vec{\theta}\right)=\sum_{k=1}^{K} w_k \cdot \frac{1}{\beta_k} \exp\left[-\exp\left(-\frac{x-\alpha_k}{\beta_k}\right)-\frac{x-\alpha_k}{\beta_k}\right]. \tag{5}$$

where u_k and $\sum_k$ are the mean value and the variance of the kth Gaussian component in the Gaussian mixture model, and a_k and β_k are the location and scale parameters of the

kth Gumbel component in the Gumbel mixture model, respectively.

2.2.2 EM algorithm-based parameter estimation

In a finite mixture model, part of the data in a certain model may not be observed, while the EM algorithm is preferred to estimate the model parameters in the case of incomplete data (McLachlan and Peel 2004, Ye *et al*. 2017) and applied hereon. The core of the EM algorithm is to calculate the optimal fitting parameters by iterating the maximum likelihood estimation from the two steps of estimating the expectation value (step E) and the maximization value (step M). Next, the parameter estimation using the EM algorithm is illustrated based on the Gaussian mixture model. The procedures are also applicable to the Gumbel mixture model.

For the given dataset, X, that are generated from a Gaussian mixture model as described in Eq. (4), a new K-dimensional random variable, z, is introduced as follows.

$$p\left(z_k=1\right)=w_k. \tag{6}$$

$$p\left(x \mid z_k=1\right)=\mathcal{N}\left(x \mid \mu_k,\Sigma_k\right). \tag{7}$$

where z_k represents whether the kth Gaussian distribution component is selected, and it has a binary value of 0 or 1; $p(z)$ is the prior probability; $p(x|z)$ is the likelihood probability. Therefore, the posterior probability $p(z|x)$ of the kth component, $r(z_k)$, can be expressed as follows.

$$\begin{aligned} r\left(z_k\right)&=p\left(z_k=1 \mid x\right)=\frac{p\left(z_k=1\right)p\left(x \mid z_k=1\right)}{p\left(x,z_k=1\right)} \\ &=\frac{w_k\mathcal{N}\left(x \mid \mu_k,\Sigma_k\right)}{\sum_{j=1}^{K} w_j\mathcal{N}\left(x \mid \mu_j,\Sigma_j\right)}. \end{aligned} \tag{8}$$

For the Gaussian mixture model, the objective of the EM algorithm is to calculate the maximum likelihood function $L(\vec{\theta})$=argmax $f(x|\vec{\theta})$. The optimization of the estimated parameters is described as follows.

$$\begin{cases} w_k=\dfrac{N_k}{N}=\dfrac{1}{N}\sum_{n=1}^{N} r\left(z_{nk}\right) \\ \mu_k=\dfrac{1}{N_k}\sum_{n=1}^{N} r\left(z_{nk}\right)\cdot x_n \\ \Sigma_k=\dfrac{1}{N_k}\sum_{n=1}^{N} r\left(z_{nk}\right)\left(x_n-\mu_k\right)\left(x_n-\mu_k\right)^T \end{cases}. \tag{9}$$

where N is the sample size of X.

Therefore, the EM algorithm can be employed to determine the optimal estimation of the Gaussian mixture model following four steps: (1) Initialization: define the number of components used, K, and set the initial values of w_k, μ_k and $\sum_k$ for each component k; (2) Expectation (step E): calculate the posterior probability, $r(z_k)$, based on w_k, u_k and $\sum_k$ using Eq. (8); (3) Maximization (step M): recalculate these parameters using $r(z_{nk})$ according to Eq. (9); (4) Convergence: repeat steps E and M until $\|\vec{\theta}^{new}-\vec{\theta}\|<\varepsilon$, where ε is the iteration tolerance.

2.2.3 Optimal clustering using AIC

In the EM algorithm, the estimation of parameters in a finite mixture model depends on the posterior information, i.e., the number of selected components, K. For any given K, the optimal parameters can be determined using the EM algorithm, but they are not necessarily the optimal solution for the observed data. The more components are used, the more accurate the finite mixture model reflects the observed data. However, the resulting model is unnecessarily complex and may be overfitting. Therefore, it is critical to determine the optimum K for the finite mixture model. Akaike (1998) provides a method for selecting the optimal fitting model to describe the observed data, which is used here as AIC=2K-ln$L(x|K,\vec{\theta})$, where K is the number of used components and ln$L(x|K,\vec{\theta})$ is the maximized value of the likelihood function for the estimated finite mixture model using K components. With the selection of different K values, the finite mixture model that produces the minimum AIC value is regarded as the optimal one. Therefore, with the optimal fitting of the finite mixture model to non-identical samples, any value $X_i(i=1,2,\ldots,N)$ can be clustered into its corresponding kth subsample if Eq. (10) is satisfied.

$$\frac{\sum_{j=1}^{k-1} w_j\cdot f_j\left(X_i\right)}{\sum_{j=1}^{K} w_j\cdot f_j\left(X_i\right)}<q\leqslant\frac{\sum_{j=1}^{k} w_j\cdot f_j\left(X_i\right)}{\sum_{j=1}^{K} w_j\cdot f_j\left(X_i\right)}. \tag{10}$$

where q is a uniformly generated random variable between 0 and 1.

2.3 Composite extreme value modelling

With initial non-identical samples clustered into iid subsamples, the traditional EVT can be successfully employed to find the limit distribution of each subsample. Gomes and Vickery (1978) first reported this observation but without deriving the equations when applying the BM-based GEV fitting. Caprani *et al*. (2008) provided the theoretical deduction of the composite extreme modeling function based on the same mathematical problem. Motivated by these works, Zhou *et al*. (2016) proposed the mixture peaks-over-threshold approach in Eq. (2), which used separated thresholds for each loading event (i.e., model component) and combined them together. This approach, similar to that proposed by Caprani *et al*. (2008), solves the problems associated with realistic structural LEs with non-identical distribution that the classical EVT cannot be directly employed to solve. However, the equation form is rather complex because the optimal threshold for each model component may be different.

However, our recent study (Zhou *et al*. 2018a) showed that if a joint threshold, u, of all model components is used, the probability distribution function of excesses, y=X-u, from Eq. (2) can be further simplified to Eq. (11).

$$\begin{aligned} F_u\left(y\right)&=\frac{F\left(y+u\right)-F\left(u\right)}{1-F\left(u\right)}=\frac{1-P\left(X>x\right)-F\left(u\right)}{1-F\left(u\right)} \\ &=\frac{\sum_{k=1}^{K} w_k G_k\left(x;\xi_k,u,\sigma_k\right)\left[1-F_k\left(u\right)\right]}{1-F\left(u\right)} \\ &=\sum_{k=1}^{K} g_k G_k\left(x;\xi_k,u,\sigma_k\right). \end{aligned} \tag{11}$$

where $g_k=w_k[1-F_k(u)]/[1-F(u)]$.

The final expression of the composite extreme prediction function (Eq. (11)) is clear and simple; g_k is the ratio of the number of exceeding data of the kth subsample to that of all subsamples based on the joint threshold. Therefore, the composite extreme prediction model is the sum of the weighted GPD models of the clustered iid subsamples. The simplified equation implies that many appropriate POT-based tail approaching models (not limited to GPD) can be used to approximate the tail of the mixture data, and its form for composite extreme extrapolation is simply the sum of the weighted models based on the joint threshold. For example, one can (if appropriate) use normal distribution to approach the tail of the real data, and the prediction equation will be the composite left truncated normal distribution.

The critical feature of the above derivation is that a joint threshold can be found for all subsamples, where the estimated shape and scale parameters for each subsample are still optimal using the joint threshold. In the search of the optimal threshold for a GPD model, the shape parameter does not change with the threshold, and the scale parameter has a close relationship with the threshold such that $\sigma'=\sigma+\xi(u'-u)$, where $u'$and $\sigma'$are the new threshold and the scale parameter, respectively. Therefore, the maximum of all the optimal thresholds for each subsample can be used as the joint threshold, and the re-estimated shape and scale parameters for each subsample based on the joint threshold are still optimal.

The common problem for the joint threshold-based composite extreme value prediction equation is the determination of the three parameters in the GPD model. It is noted there are many algorithms for the parameter estimation of the GPD model, especially for threshold selection (Lang et al. 1999; Scarrott and MacDonald 2012). In the study, the following procedures are recommended to find the solution: (1) Set the initial threshold that starts from the value of the maximal probability density to the maximum of the kth subsamples; (2) Use the method of probability weighted moment (PWM) to estimate ξ_k and σ_k in the kth subsample considering the limited number of POT (Bermudez and Kotz 2010); (3) Employ the Kolmogorov-Smirnov (K-S) test, a computational approach, to determine whether the threshold is optimal by minimizing the fitting error; (4) Repeat the above steps to find the optimal threshold for the subsample, and the joint threshold is the maximum of these components, i.e., $u=\max\{u_1, u_2,\ldots,u_k\}$.

3. Numerical examples

Numerical examples with given functions have known solutions to the predicted extreme of any reference period and therefore are used here for verification. The parameters of the numerical examples are shown in Table 1. The sample size per day is 3000, and 1000 days are simulated. The underlying data are generated by the known Gaussian mixture model or the Gumbel mixture model so that the theoretical extreme of any reference period can be easily calculated using Eq. (12).

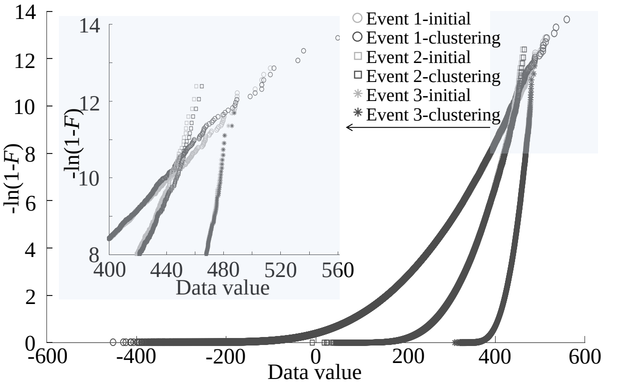

Fig. 2 Comparison between initial data and clustered data: an example of the numerical example 3 using the Gaussian mixture model (referring to Table 1).

$$P(X\leqslant x)=\prod_{i=1}^{N}\left(\sum_{k=1}^{K}w_k\cdot F_k(x)\right)=\left(\sum_{k=1}^{K}w_k\cdot F_k(x)\right)^N. \quad (12)$$

where N is the sample size of X in the specified reference period.

3.1 Verification of clustering

Initial samples of each example are generated using the given parameters of the finite mixture model. The EM algorithm and AIC are then applied to estimate the parameters for fitting the finite mixture model. Finally, the initial data are clustered into subsamples using Eq. (10). As shown in Table 1, the estimated parameters show good agreement with the given data, where R^2 for each example is larger than 0.9999. To illustrate the agreement between the clustering data and the initial data, example 3 of the Gaussian mixture model (Table 1) is demonstrated in Fig. 2. It is known from Fig. 2 that the clustering data are the same as the initial data of each model component (i.e., event type), and the tail tendencies are also consistent. Similar results are found in other numerical examples. Therefore, POT-based GPD can be applied to the clustered subsamples.

3.2 Validation of extrapolation

The fitting parameters of the GPD model for each event type are calculated using the K-S test and the PWM method (Table 2). The results of the Gaussian mixture model are only shown for the validation of the composite extreme value model using clustering, which is the proposed approach. The classical EVT fitting using the mixture POT that ignores the iid assumption is also studied for comparison, which is the conventional approach. For comparison, the joint threshold used in the proposed approach is also employed for the conventional approach, and the scale parameter is transformed from its estimated optimal threshold. With all the estimated parameters, the extracted data of POT from each event type together with their fitting models are plotted in Fig. 3. The sample sizes for each event and the mixture are different, indicating that the same vertical coordinate of each fit line in Fig. 3

Table 1 Given and estimated parameters in numerical examples.

Example No.	Sample size per day	Event No.	Gaussian mixture model			Gumbel mixture model		
			Given ($w, \mu, \sqrt{\Sigma}$)	Estimated ($w, \mu, \sqrt{\Sigma}$)	R^2	Given (w, α, β)	Estimated (w, α, β)	R^2
1	3000	1	(0.5, 60, 100)	(0.50, 59.99, 101.54)	0.99999	(0.5, 50, 3)	(0.50, 50.02, 3.00)	0.99998
		2	(0.5, 50, 90)	(0.50, 50.17, 89.39)		(0.5, 45, 2)	(0.50, 45.02, 2.01)	
2	3000	1	(0.9, 50, 100)	(0.90, 49.95, 100.14)	0.99998	(0.9, 42, 3)	(0.90, 42.00, 3.00)	0.99998
		2	(0.1, 260, 60)	(0.10, 260.23, 60.11)		(0.1, 50, 2)	(0.10, 50.01, 2.00)	
3	3000	1	(0.7, 50, 100)	(0.70, 50.12, 100.24)	0.99996	(0.7, 42, 3)	(0.70, 42.00, 3.00)	0.99997
		2	(0.2, 250, 50)	(0.20, 249.96, 50.06)		(0.2, 50, 2)	(0.20, 50.02, 2.01)	
		3	(0.1, 400, 20)	(0.10, 400.09, 20.05)		(0.1, 54, 1)	(0.10, 53.48, 1.00)	

Table 2 The estimated parameters of the proposed and conventional approaches from the numerical examples of Gaussian mixture models.

Example No.	Event No.	Approach type	Weight, w	Threshold, u	Shape parameter, ξ	Scale parameter, σ
1	1	Proposed	0.86	388.60	-0.0359	27.85
	2		0.14		-0.3089	29.15
	N/A	Conventional	1.00		-0.0357	27.35
2	1	Proposed	0.16	384.21	-0.0343	27.00
	2		0.84		-0.1034	24.29
	N/A	Conventional	1.00		-0.0812	24.49
3	1	Proposed	<0.01	402.71	-0.0322	26.40
	2		<0.01		-0.0601	14.46
	3		0.99		-0.1819	17.50
	N/A	Conventional	1.00		-0.1539	16.28

represents different levels of return period. Fig. 3 also shows the plots of the data for each event type and the mixture without clustering. The changing regulations of the prediction results using the proposed and conventional approach, and their relationship with each event type are also presented.

Three numerical examples with known solutions are demonstrated to validate the benefit of clustering and the joint threshold for the proposed composite extreme value modeling. Example 1 shows the non-identical data composited by two Gaussian components of equal weight. Event 1 has a larger location parameter and a greater scale parameter, while Event 2 has a lower location parameter and a smaller scale parameter. Event 1 has a longer tail and a greater proportion of tailed data, governing the extreme in the high-return period as shown in Fig. 3(a), where prediction results using the proposed approach with clustering nearly coincides with those of Event 1. Moreover, differences in the predicted values obtained using the proposed and the conventional approach are small because the data of POT are mainly from Event 1. Example 2 shows the non-identical data also formed by two Gaussian components but with different weights, where Event 1 has a lower location parameter but a greater scale parameter and Event 2 has a larger location parameter but a smaller scale parameter. Event 1 has a longer tail but its proportion contributing to POT is small. Fig. 3 (b) shows that prediction results using the proposed approach changes along the trend of Event 2 in the lower part but shifts to the trend of Event 1 in the upper part; the extreme in the high-return period is governed by Event 1. Significant differences in the values predicted using the proposed and the conventional approach are detected in example 2 because the POT data are the mixture of Event 1 and 2; thus, the model fit using the conventional approach on the data does not well describe the tail tendency. Example 3 adds a Gaussian component (Event 3) with the largest location parameter but the smallest scale parameter based on Example 2. The fitting results using the proposed approach changes along the trend of Event 3 in the lower part and then curves to the trend of Event 1 in the upper part, and the differences between the proposed and conventional approaches are significant (Fig. 3(c)).

Fig. 4 shows the comparison of the predicted extrema under various return periods using the proposed and conventional approaches. The cumulative probabilities for the POT method are P=1-1/(365 × T × n_{POT}), where T is the return period and n_{POT} is the average daily number of data points exceeding the threshold. The theoretical value (known solution) is derived from the known distribution equations following Eq. (12). When the tailed data are generated by a certain Gaussian component, e.g., Example 1, predictions using the proposed and the conventional approaches yield the same results. However, if the tailed data are a mixture of several Gaussian components, the predicted extrema using the two approaches are

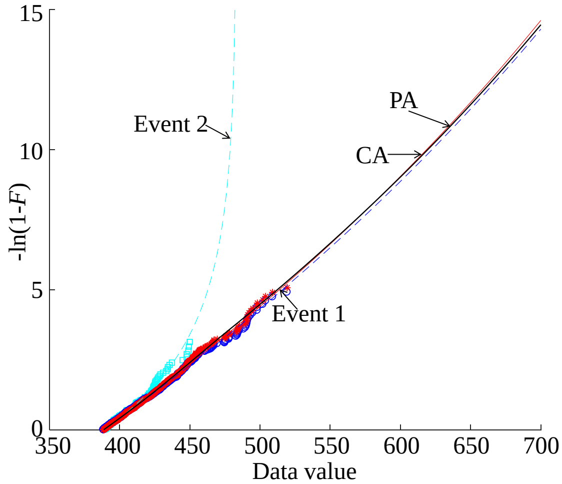

(a) Example 1

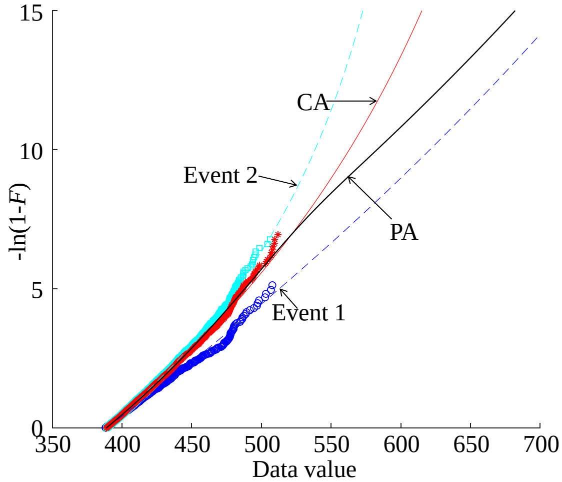

(b) Example 2

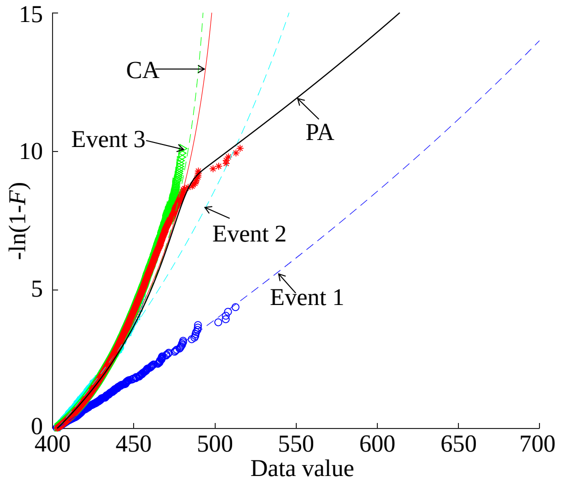

(c) Example 3

Fig. 3 Probability paper plot of extrapolation data and their fitting distributions (PA: the proposed approach, CA: the conventional approach)

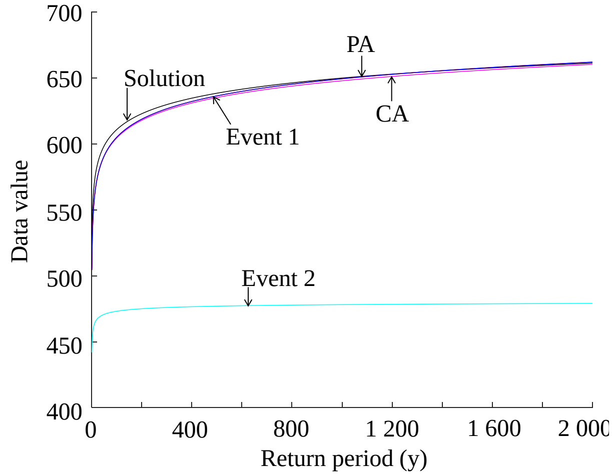

(a) Example 1

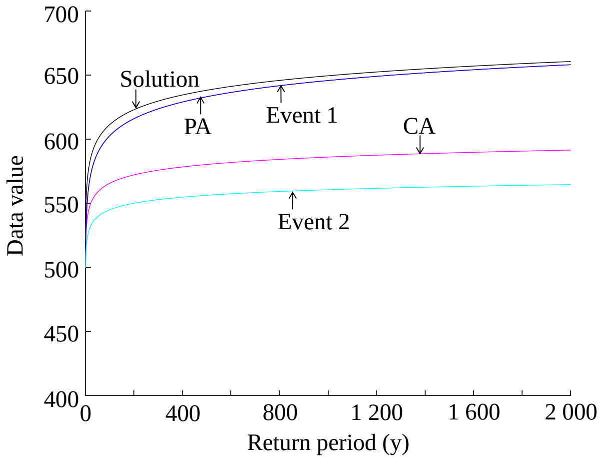

(b) Example 2

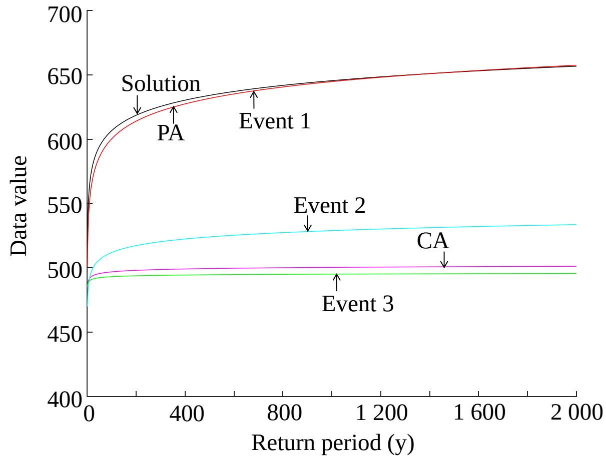

(c) Example 3

Fig. 4 Comparison of predicted extrema using the proposed and conventional approaches (PA: the proposed approach, CA: the conventional approach)

significantly different, e.g., Examples 2 and 3. Under these conditions, the proposed approach yields more accurate results, with a relative error of less than 1%, whereas the conventional approach yields a relative error up to 24% (Fig. 4(c)).

The predicted extrema in long reference periods using the proposed approach are determined by the model component that governs the tailed data in the finite mixture model. One can directly employ a certain distribution

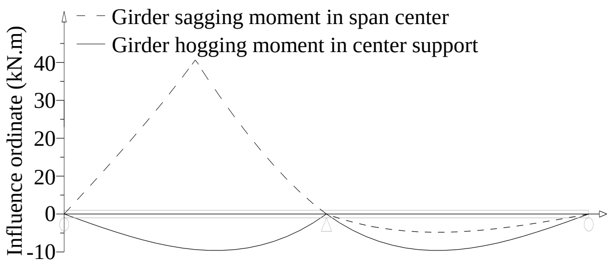

Fig. 5 Layout of the case bridge and influence lines

function to approximate the tail of the empirical cumulative distribution of the underlying data, such as the straight-line inference using a Gaussian or Gumbel probability paper. If the underlying data can be clustered by a finite mixture model, then the subsamples from the model component that governs the tail tendency of the underlying data can be selected for extrapolation.

Therefore, numerical studies verify that the composite extreme value model using clustering can address the prediction problem of non-identical samples and yield consistent results with theoretical solutions.

4. Engineering application

Application of the proposed approach to structural LEs of traffic loading on a long-span bridge is demonstrated in this section. A two-span continuous girder bridge with a constant section and equal span of 200 m is studied. The bridge is assumed to carry two-lane unidirectional traffic. The continuous bridge type assumed here is to illustrate the influence lines (ILs) of long-span bridges in terms of positive and negative lobes, similar to that of (Guo and Caprani 2018). To calculate bridge LEs under stochastic traffic flow, the linear superposition method is employed between vehicle load sequences and the ordinates of influence lines, where an IL is the graph of responses of a certain structural effect caused by a moving unit point load along the bridge span in a traffic lane. Two critical ILs of the bridge are investigated. One is the girder hogging moment in the center support, denoted by IL1. The other is the girder sagging moment in the span center, denoted by IL2. Fig. 5 shows the bridge and the two ILs, where the IL ordinates are derived based on the unit point load of 1 kN.

To present how the proposed approach is applied to extrapolate the extreme traffic LE of the studied bridge, it is important to acquire adverse underlying traffic LEs over the bridge lifetime, which is difficult to measure because onerous traffic loading scenarios of long-span bridges are very rare in daily life. To address this concern, traffic simulation is performed to trigger adverse traffic LEs of the two ILs during the bridge lifetime. Using the time-history of LEs, the proposed clustering methods are applied and individual subsamples that accord with the iid assumption are extracted. Finally, the composite extreme prediction equation is applied to predict the characteristic bridge LEs.

4.1 Simulation of bridge traffic loading

Over the service life of a long-span bridge, there are many traffic loading events, and free flow and congestion are the two fundamental ones. However, free flow may vary depending on the situation such as high traffic volume but low truck proportion in the daytime and low traffic volume but high truck proportion in the nighttime (Ruan *et al.* 2017b; Zhou *et al.* 2018b). Moreover, congestion can take several forms such as full stop traffic, stop and go waves, and homogeneous traffic congestion (Guo and Caprani 2018). To model the real-world traffic loading over a long distance, the microscopic behavior of vehicles, such as car-following and lane-changing, should be considered, which is known as traffic microsimulation. Herein, a novel cellular automaton-based traffic microsimulation, known as multi-axle single-cell cellular automaton (MSCA), is used to model the traffic action on bridges (Ruan *et al.* 2017b). MSCA can generate accurate axle load sequences for bridge loading and is verified using the weigh-in-motion (WIM) data. Furthermore, two-lane unidirectional WIM data are utilized as the basis for the traffic microsimulation on the bridge. For further information on the WIM data, readers are referred to (Ruan *et al.* 2017b).

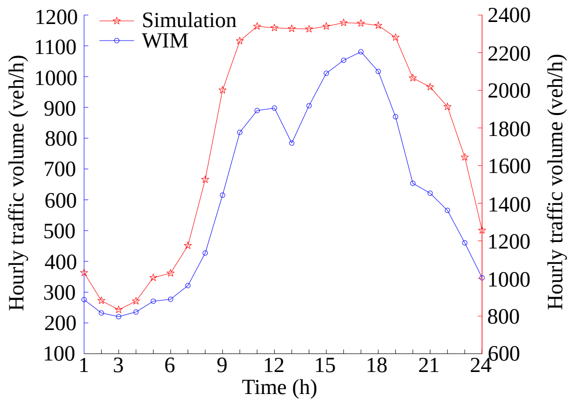

Fig. 6 Hourly traffic volume from WIM data and traffic microsimulation

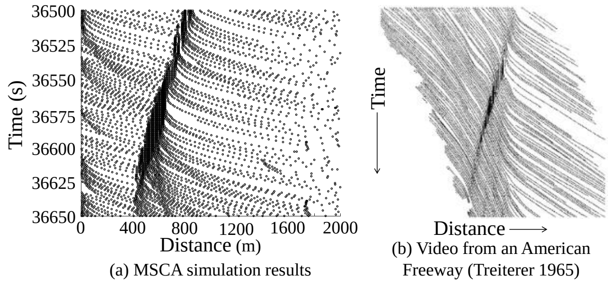

Fig. 7 Comparison of congested traffic between (a) simulations and (b) observations

The WIM data used here reflect the free-flow conditions with a medium volume of 20,373 vehicles per day including cars. However, the bridge may undertake much higher traffic volumes and thus severe LEs. In order to present the most severe LEs over the bridge's service life, the average daily traffic volume in the simulation is amplified based on the hourly traffic volume regulations of the WIM data to trigger congestion. In the microsimulation by the MSCA, the random deceleration factor is set as 0.5 and the lane-changing probabilities are set as 1.0. Finally, a relative high volume of 42,526 vehicles per day is generated. The changing regulation of hourly traffic volume of the

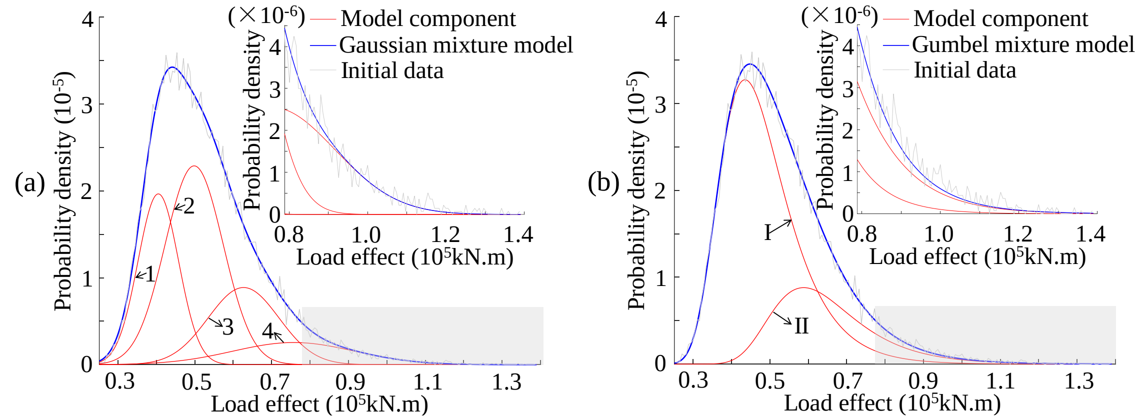

Fig. 8 Fitting and clustering on traffic LEs of IL1 with (a) a Gaussian mixture model and (b) a Gumbel mixture model

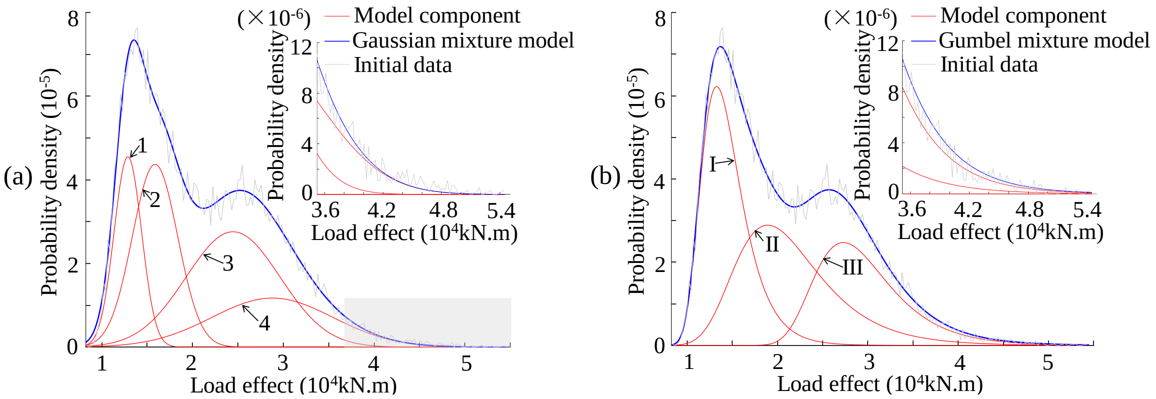

Fig. 9 Fitting and clustering on traffic LEs of IL2 with (a) a Gaussian mixture model and (b) a Gumbel mixture model

simulation is shown in Fig. 6, together with that of WIM data. In Fig. 6, the peaks in the hourly traffic volume of the WIM data show the rush hour traffic at 16:00–17:00. However, in the simulation, congestion occurs between 10:00 and 18:00, as evidenced by the horizontal hourly traffic volume over time, indicating that the road capacity has been reached.

Fig. 7(a) shows the space versus time information of the simulated traffic in the fast lane; dotted points represent vehicles. The horizontal axis represents the physical location of each vehicle on the road, and the vertical axis is the time range. Congestion is illustrated by the black belts in Fig. 7(a), which is consistent with the observed traffic phenomenon from the video records of an American freeway, Fig. 7(b) (Treiterer 1965).

4.2 Clustering of bridge LEs

In the microsimulation, free flow in the nighttime with high truck proportion and congested flow in the daytime with low truck proportion are modeled, which represents the adverse traffic loading events over the bridge's service life. On the bridge, 1000-day traffic with a time step of 0.2 s is simulated, and the history of LEs on two ILs is obtained. The vehicle-bridge coupling vibration is significant under free-flow conditions but very low under traffic congestion. Hence, a dynamic impact factor should be added to the simulated load effects under free-flow conditions. Herein, a dynamic impact factor of 0.05 recommended for long-span bridges (MCT 2015) is used.

The bridge LEs from the microsimulations are driven by multiple events; therefore, they require clustering. There are many components of the finite mixture model to accurately model the data if all the LEs are used because small LEs with a large proportion affect the fitting and clustering results of tailed LEs. Therefore, hourly maximal LEs are extracted as the initial data to filter these small and negligible LEs. Consequently, the tailed LEs can be properly modeled using a finite mixture model, and these initial data can be regarded as independent. These picked LEs belong to both the congested and free-flow traffic conditions, but the congested LEs contribute over 85%. To investigate the sensitivity of the finite mixture model used, Gaussian and Gumbel mixture models are synchronously studied and compared.

Figs. 8 and 9 show the fitting and clustering of traffic LEs of IL1 and IL2 with a Gaussian mixture model and a Gumbel mixture model. These estimated parameters are presented in Table 3. The fitted Gaussian mixture model and the Gumbel mixture model both describe the empirical probability density distribution of the initial data with R^2 >0.999, and the tailed LEs are well captured. A smaller number of model components are used for effective clustering in the Gumbel mixture model than in the Gaussian mixture model. With the finite mixture model, all the initial data can be clustered into their corresponding model components.

4.3 Prediction of characteristic LEs

The trends in LEs in components 1 and 2 of the

Table 3 Estimated parameters of the finite mixture models on bridge traffic LEs

Bridge effect	Gaussian mixture model					Gumbel mixture model				
	Component No.	w	μ (10^4kN.m)	$\sqrt{\Sigma}$ (10^3kN.m)	R^2	Component No.	w	α (10^4kN.m)	β (10^3kN.m)	R^2
IL1	1	0.26	4.05	5.29	0.99994	I	0.74	4.35	8.37	0.99985
	2	0.43	4.98	7.55		II	0.26	5.88	10.68	
	3	0.21	6.27	9.22		N/A				
	4	0.10	7.58	15.92						
IL2	1	0.17	1.29	1.51	0.99982	I	0.37	1.33	2.17	0.99993
	2	0.27	1.59	2.50		II	0.36	1.89	4.58	
	3	0.36	2.45	5.18		III	0.27	2.73	4.08	
	4	0.20	2.88	6.66		N/A				

Table 4 Estimated parameters using the proposed and conventional approaches for the studied case

Bridge effect	Approach type [a]	μ (10^4kN.m)	Gaussian mixture model				Gumbel mixture model			
			Component No.	w	ξ	σ (103kN.m)	Component No.	w	ξ	σ (10^3kN.m)
IL1	PA	7.88	3	0.15	-0.1728	4.13	I	0.23	-0.1254	9.58
			4	0.85	-0.1779	15.41	II	0.77	-0.1496	14.05
	CA		N/A	1.00	-0.1081	12.73	N/A	1.00	-0.1081	12.73
IL2	PA	3.52	3	0.17	-0.1735	2.43	II	0.24	-0.2224	5.08
			4	0.83	-0.1375	5.19	III	0.76	-0.0966	4.28
	CA		N/A	1.00	-0.0869	4.44	N/A	1.00	-0.0869	4.44

Note: [a] PA: the proposed approach; CA: the conventional approach

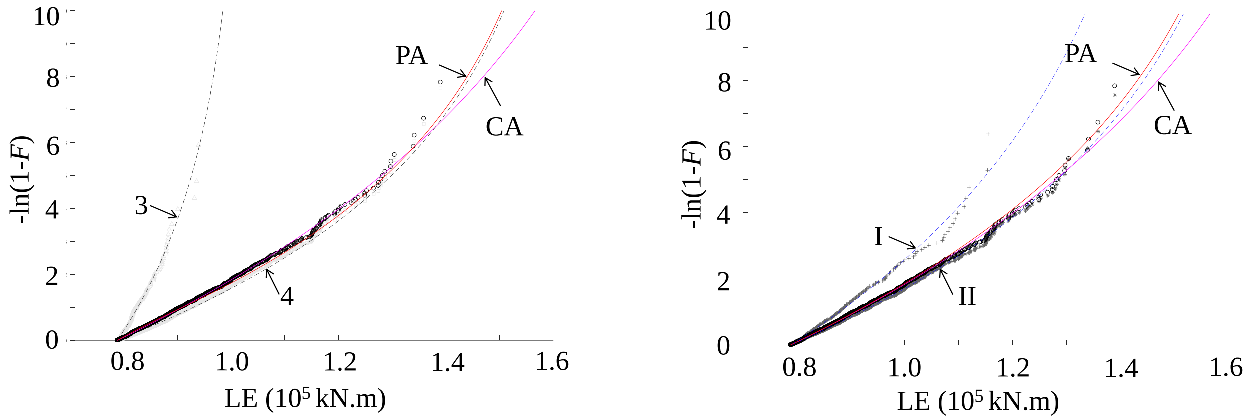

(a) Gaussian mixture model (b) Gumbel mixture model

Fig. 10 Comparison of LEs of IL1 using the proposed approach (PA) and the conventional approach (CA)

Gaussian mixture models for IL1 and IL2 curve upward, and similar results are detected in LEs of component I of the Gumbel mixture model for IL1. These model components have very little impact on the prediction of the extrema because they produce low-magnitude LEs. Therefore, only contributive component-LEs are plotted in Figs. 10 and 11 together with the fitting models of components and the composite prediction equation. The estimated parameters are listed in Table 4 where a joint threshold is used for the proposed and conventional approaches of the Gaussian mixture model and the Gumbel mixture model. In the results of the Gaussian mixture model, only components 3 and 4 influence the extreme extrapolation of LEs, and the tail tendency of LEs is more likely to be influenced by component 4 than by component 3 both for IL1 and IL2. The values predicted by the Gumbel mixture model in short evaluation periods are concurrently influenced by two model components, but mainly governed by the last model component in the high-return period. Moreover, the estimations using both approaches well describe the global data. However, the proposed approach more accurately captures the maximal outliers as indicated in Figs. 10 and 11 where it curves more significantly to these outliers. Furthermore, the Gumbel mixture model is

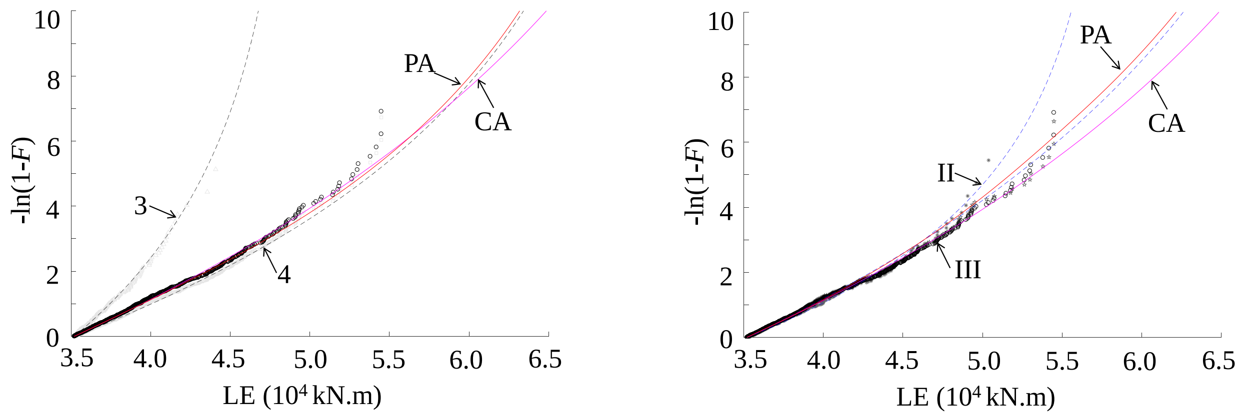

(a) Gaussian mixture model (b) Gumbel mixture model

Fig. 11 Comparison of LEs of IL2 using the proposed approach (PA) and the conventional approach (CA)

Table 5 Comparison of predicted characteristic LEs using the proposed and conventional approaches

Bridge effect	Return period (y)	CA (10^5kN.m)	Gaussian mixture model		Gumbel mixture model		RE[3](%)
			PA (10^5kN.m)	RE[1](%)	PA (10^5kN.m)	RE[2](%)	
IL1	5	1.455	1.430	1.748	1.420	2.465	0.699
	20	1.526	1.479	3.178	1.478	3.248	0.068
	100	1.597	1.523	4.859	1.531	4.311	0.525
	500	1.656	1.555	6.495	1.573	5.277	1.158
	1000	1.678	1.567	7.084	1.588	5.668	1.340
	2000	1.699	1.577	7.736	1.602	6.055	1.585
IL2	5	0.597	0.592	0.845	0.585	2.051	1.182
	20	0.627	0.616	1.786	0.612	2.451	0.649
	100	0.658	0.638	3.135	0.630	4.444	1.254
	500	0.685	0.656	4.421	0.654	4.740	0.305
	1000	0.695	0.663	4.827	0.663	4.827	0.010
	2000	0.705	0.669	5.381	0.671	5.067	0.299

Note: PA-the proposed approach, CA-the conventional approach; [1] relative error of CA to PA using Gaussian mixture model; [2] relative error of CA to PA using Gumbel mixture model; [3] relative error of PA using Gumbel mixture model to PA using Gaussian mixture model.

more effective than the Gaussian mixture model in capturing these outliers. Therefore, the composite extreme value model produces more accurate fitting results on the tailed LEs, and the conventional prediction method yields deviations especially for the evaluation of characteristic LEs in high-return periods.

Table 5 presents the comparison of characteristic LEs in several typical return periods predicted using the proposed and conventional approaches. The predicted extrema of the proposed approach using the Gaussian and the Gumbel mixture models are in good agreement with a relative error of less than 2%. However, the results of the conventional approach show an up to 8% relative error compared to those of the proposed approach, and the error grows with the return period. The real-world bridge traffic LEs are driven by multiple events, and conventional extrapolation approach that ignores the iid assumption may produce large deviations in the prediction of extreme values, especially for long return periods. However, the proposed composite extreme value modeling approach generates much accurate results. Furthermore, provided that underlying data can be well clustered by the finite mixture model, the choice of the type of the finite mixture model slightly influences the prediction results, but Gumbel mixture model is still recommended because it more capable of capturing outliers of tailed structural LEs.

5. Conclusion

Composite extreme value modeling approach using clustering is proposed to address the prediction problems of structural LEs that are driven by multiple events thus not identically distributed. The finite mixture model, EM algorithm, and AIC are employed to cluster the initial mixture data into several subsamples that follow an identical distribution. POT-based GPD is applied to build the limit distribution of each subsample. The limit distributions are combined to form the composite extreme value modeling equation using a joint threshold. Numerical examples with known solutions are used to validate the approach. Engineering application of the approach into the prediction of characteristic bridge traffic LEs is demonstrated on a long-span bridge. Main findings include the following:

(1) A joint threshold largely benefits the clustering-based composite extreme value modeling of non-identical samples using the POT theory, which highlights that many appropriate tail approaching models can be used to approximate the tail of the mixture samples, and its composite extrapolation equation is simply the sum of the weighted models based on the joint threshold.

(2) Numerical examples verify that the proposed approach is effective in classifying the mixture samples into several iid subsamples, and can give accurate predictions on the extrema of any reference period compared to the known solutions. However, the conventional approach that ignores the non-identical assumption produces large deviations.

(3) Engineering application indicates the proposed approach shows good agreement with the tail tendency of LEs, whereas the conventional approach produces large relative deviations, especially in high-return periods. The predicted extrema using the Gaussian mixture model and the Gumbel mixture model are in good agreement, indicating that the choice of the type of the finite mixture model slightly affects the prediction accuracy. However, the Gumbel mixture model is recommended because it is more capable of capturing the outliers of tailed structural LEs.

The findings of the engineering application are based on the specific case study in the work and may show some bias in other cases. Nevertheless, the proposed composite extreme value modeling approach should find wide applications to general problems such as samples that are driven by multiple events and that do not accord with the identical distribution assumption in extrapolation. Furthermore, the approach can be extended to composite multivariate extreme value modeling.

Acknowledgments

This work was supported by National Nature Science Foundation of China [grant number 51808148]; Natural Science Foundation of Guangdong Province, China [grant number 2019A1515010701]; Science and Technology Program of Guangzhou, China [grant number 201904010188].

References

Akaike, H. (1998), "Information theory and an extension of the maximum likelihood principle", *Selected Papers of Hirotugu akaike*, Springer, New York, 199-213. https://doi.org/10.1007/978-1-4612-1694-0_15.

Au-Yong, C. P., Ali, A. S., Ahmad, F. and Chua, S. J. L. (2017). "Optimal inspection frequency to mitigate the risk of building system failure", *Struct. Eng. Mech.*, **64**(3), 347-352. https://doi.org/10.12989/sem.2017.64.3.347.

Bermudez, P. de Zea. And Kotz, S. (2010), "Parameter estimation of the generalized Pareto distribution—Part I", *J. Statistical Plan. Inference*, **140**(6), 1353-1373. https://doi.org/10.1016/j.jspi.2008.11.019.

Caprani, C. C. (2012), "Lifetime highway bridge traffic load effect from a combination of traffic states allowing for dynamic amplification", *J. Bridge Eng.*, **18**(9), 901-909. https://doi.org/10.1061/(ASCE)BE.1943-5592.0000427.

Caprani, C. C., O'Brien, E. J. and McLachlan, G. J. (2008), "Characteristic traffic load effects from a mixture of loading events on short to medium span bridges", *Structural Safety*, **30**(5), 394-404. https://doi.org/10.1016/j.strusafe.2006.11.006.

Cook, N. J. (2004), "Confidence limits for extreme wind speeds in mixed climates", *J. Wind Eng. Industrial Aerodynam.*, **92**(1), 41-51. https://doi.org/10.1016/j.jweia.2003.09.037.

Davison, A. C. and Smith, R. L. (1990). "Models for exceedances over high thresholds", *J. Royal Statistical Soc. B (Methodological)*, **52**(3), 393-442. https://doi.org/10.1111/j.2517-6161.1990.tb01796.x.

Easterling, D. R., Meehl, G. A., Parmesan, C., Changnon, S. A., Karl, T. R. and Mearns, L. O. (2000) "Climate extremes: observations, modeling, and impacts", *Science*, **289**(5487), 2068-2074. https://doi.org/10.1126/science.289.5487.2068.

EC1. (2003), *Actions on structures. Part* 2: *Traffic loads on bridges*. *Eurocode* 1, *EN* 1991-2:2003, European Committee for Standardization, Brussels.

Frangopol, D. M. and Liu, M. (2007), "Maintenance and management of civil infrastructure based on condition, safety, optimization, and life-cycle cost", *Struct. Infrastruct. Eng.*, **3**(1), 29-41. https://doi.org/10.1080/15732470500253164.

Gomes, L. and Vickery, B. J. (1978), "Extreme wind speeds in mixed climates", *J. Wind Eng. Industrial Aerodynam.*, **2**(4), 331-344. https://doi.org/10.1016/S0167-6105(02)00397-5.

Gumbel, E. J. (2012). *Statistics of Extremes*, Dover Publications, Inc., Mineola, New York, U.S.A.

Guo, D. and Caprani, C. C. (2018), "Traffic load patterning on long span bridges: A rational approach", *Structural Safety*, **77**, 18-29. https://doi.org/10.1016/j.strusafe.2018.11.003.

Jeong, Y. J., Park, M. S., and You, Y. J. (2016), "Experimental study on wave forces to offshore support structures", *Struct. Eng. Mech.*, **60**(2), 193-209. https://doi.org/10.12989/sem.2016.60.2.193.

Lang, M., Ouarda, T. B. M. J. and Bobée, B. (1999), "Towards operational guidelines for over-threshold modeling", *J. Hydrology*, **225**(3-4), 103-117. https://doi.org/10.1016/S0022-1694(99)00167-5.

McLachlan, G. and Peel, D. (2004). *Finite Mixture Models*, John Wiley & Sons, New Jersey, U.S.A.

Ministry of Communications and Transportation (MCT) (2015), *General code for design of highway bridges and culverts JTG D60-2015*, China Communications Press, Beijing, China. (In Chinese).

Rivas, D., Caleyo, F., Valor, A. and Hallen, J. M. (2008), "Extreme value analysis applied to pitting corrosion experiments in low carbon steel: comparison of block maxima and peak over threshold approaches", *Corrosion Sci.*, **50**(11), 3193-3204.

Madsen, H. Rasmussen, P.F. and Rosbjerg, D. (1997), "Comparison of annual maximum series and partial duration series methods for modeling extreme hydrologic events: 1. At-site modeling", *Water Resources Res.*, **33**(4), 747-757. https://doi.org/10.1029/96WR03848.

Ruan, X., Zhou, J. Y., Shi, X. F. and Caprani, C. C. (2017a), "A site-specific traffic load model for long-span multi-pylon cable-stayed bridges", *Struct. Infrastruct. Eng.*, **13**(4), 494-504. https://doi.org/10.1080/15732479.2016.1164724.

Ruan, X., Zhou, J. Y., Tu, H. Z., Jin, Z. R. and Shi, X. F. (2017b), "An improved cellular automaton with axis information for microscopic traffic simulation", *Transport. Res. Part C Emerg. Technol.*, **78**, 63-77. https://doi.org/10.1016/j.trc.2017.02.023.

Scarrott, C. and MacDonald, A. (2012), "A review of extreme value threshold estimation and uncertainty quantification", *REVSTAT–Statistical J.*, **10**(1), 33-60.

Tabsh, S. W. and Mitchell, M. M. (2016), "Girder distribution factors for steel bridges subjected to permit truck or super load", *Struct. Eng. Mech.*, **60**(2), 237-249. https://doi.org/10.12989/sem.2016.60.2.237.

Treiterer, J. (1965), *Investigation and Measurement of Traffic Dynamics, Appendix IX to Final Report EES 202-2*, Ohio State University, U.S.A.

Xia, Y. X., and Ni, Y. Q. (2016), "Extrapolation of extreme traffic load effects on bridges based on long-term SHM data", *Smart Struct. Syst.*, **17**(6), 995-1015. https://doi.org/10.12989/sss.2016.17.6.995.

Ye, X. W., Xi, P. S., Su, Y. H. and Chen, B. (2017). "Analysis and probabilistic modeling of wind characteristics of an arch bridge using structural health monitoring data during typhoons", *Struct. Eng. Mech.*, **63**(6), 809-824. https://doi.org/10.12989/sem.2017.63.6.809.

Zhang, S., Solari, G., Yang, Q. and Repetto, M. P. (2018), "Extreme wind speed distribution in a mixed wind climate", *J. Wind Eng. Industrial Aerodynam.*, **176**, 239-253. https://doi.org/10.1016/j.jweia.2018.03.019.

Zhou, X. Y., Schmidt, F., Toutlemonde, F. and Jacob, B. (2016), "A mixture peaks over threshold approach for predicting extreme bridge traffic load effects", *Probabilistic Eng. Mech.*, **43**, 121-131. https://doi.org/10.1016/j.probengmech.2015.12.004.

Zhou, J.Y., Shi, X. F. and Ruan, X. (2018a), "Composite extrema prediction of multi-event driven bridge traffic load effects", *J. Harbin Institute Technol.*, **50**(9), 11-18. (In Chinese).

Zhou, J. Y., Shi, X. F., Caprani, C. C. and Ruan, X. (2018b). "Multi-lane factor for bridge traffic load from extreme events of coincident lane load effects", *Struct. Safety*, **72**, 17-29. https://doi.org/10.1016/j.strusafe.2017.12.002.

Zhou, J.Y., Shi, X. F., Zhang, L.W. and Sun, Z. (2019). "Traffic control technologies for component replacement of long-span bridges using microsimulation", *Struct. Eng. Mech.*, **70**(2), 169-178. https://doi.org/10.12989/sem.2019.70.2.169.

CC